

ORIGINAL ARTICLE

Dedicated Breast CT: Feasibility for Monitoring Neoadjuvant Chemotherapy Treatment

Srinivasan Vedantham, Avice M O'Connell¹, Linxi Shi, Andrew Karellas, Alissa J Huston², Kristin A Skinner³

Department of Radiology, University of Massachusetts Medical School, Worcester, Massachusetts, ¹Departments of Imaging Sciences and ²Medicine, Divisions of Hematology/Oncology and ³Surgery, University of Rochester Medical Center, Rochester, New York, USA

Address for correspondence:

Dr. Srinivasan Vedantham,
Department of Radiology,
University of Massachusetts
Medical School, 55 Lake Avenue
North, Room S2-835A, Worcester,
Massachusetts - 01655, USA.
E-mail: srinivasan.vedantham@umassmed.edu



Received : 04-08-2014

Accepted : 20-10-2014

Published : 29-11-2014

ABSTRACT

Objectives: In this prospective pilot study, the feasibility of non-contrast dedicated breast computed tomography (bCT) to determine primary tumor volume and monitor its changes during neoadjuvant chemotherapy (NAC) treatment was investigated. **Materials and Methods:** Eleven women who underwent NAC were imaged with a clinical prototype dedicated bCT system at three time points – pre-, mid-, and post-treatment. The study radiologist marked the boundary of the primary tumor from which the tumor volume was quantified. An automated algorithm was developed to quantify the primary tumor volume for comparison with radiologist's segmentation. The correlation between pre-treatment tumor volumes from bCT and MRI, and the correlation and concordance in tumor size between post-treatment bCT and pathology were determined. **Results:** Tumor volumes from automated and radiologist's segmentations were correlated (Pearson's $r = 0.935$, $P < 0.001$) and were not different over all time points [$P = 0.808$, repeated measures analysis of variance (ANOVA)]. Pre-treatment tumor volumes from MRI and bCT were correlated ($r = 0.905$, $P < 0.001$). Tumor size from post-treatment bCT was correlated with pathology ($r = 0.987$, $P = 0.002$) for invasive ductal carcinoma larger than 5 mm and the maximum difference in tumor size was 0.57 cm. The presence of biopsy clip (3 mm) limited the ability to accurately measure tumors smaller than 5 mm. All study participants were pathologically assessed to be responders, with three subjects experiencing complete pathologic response for invasive cancer and the remainder experiencing partial response. Compared to pre-treatment tumor volume, there was a statistically significant ($P = 0.0003$, paired t -test) reduction in tumor volume

at mid-treatment observed with bCT, with an average tumor volume reduction of 47%. **Conclusions:** This pilot study suggests that dedicated non-contrast bCT has the potential to serve as an expedient imaging tool for monitoring tumor volume changes during NAC. Larger studies are needed in future.

Key words: Breast, dedicated breast CT, neoadjuvant chemotherapy, tomography, tumor size

Access this article online

Quick Response Code:



Website:

www.clinicalimaging-science.org

DOI:

10.4103/2156-7514.145867

Copyright: © 2014 Vedantham S. This is an open-access article distributed under the terms of the Creative Commons Attribution License, which permits unrestricted use, distribution, and reproduction in any medium, provided the original author and source are credited.

This article may be cited as:

Vedantham S, O'Connell AM, Shi L, Karellas A, Huston AJ, Skinner KA. Dedicated Breast CT: Feasibility for Monitoring Neoadjuvant Chemotherapy Treatment. J Clin Imaging Sci 2014;4:64. Available FREE in open access from: <http://www.clinicalimaging-science.org/text.asp?2014/4/1/64/145867>

INTRODUCTION

Neoadjuvant chemotherapy (NAC) treatment for women diagnosed with local-regional disease has been shown to reduce the tumor size of most breast tumors and decrease the incidence of positive nodes.^[1] The 5- and 9-year follow-up results from the National Surgical Adjuvant Breast and Bowel Project B-18 indicate overall survival and disease-free survival were not statistically different between NAC and postoperative adjuvant therapy.^[2,3] NAC has been shown to increase breast-conserving lumpectomy rates.^[1-3] Overall survival, disease-free survival, and relapse-free survival are statistically correlated with the pathologic primary tumor response.^[3] Physical examination, ultrasound, and mammography are of limited value for predicting pathologic residual tumor size after NAC.^[4] The use of fluorodeoxyglucose positron emission tomography (FDG-PET) to provide a functional measure of NAC response has been reported.^[5,6] Breast magnetic resonance imaging (MRI) is increasingly considered as the preferred imaging modality for predicting pathologic response.^[7-9] The Translational Breast Cancer Research Consortium trial 017 observed that the tumor size from MRI had an overall accuracy of 74% in predicting complete pathologic response and it varied substantially among tumor subtypes.^[7] Another study using MRI observed that changes in tumor volume provided a more sensitive assessment than changes in tumor size.^[8] The American College of Radiology Imaging Network 6657 trial noted that tumor volume changes assessed using MRI early in the NAC cycle had an accuracy of 0.7 for predicting pathologic response.^[9] The study reported that the in-plane spatial resolution for contrast-enhanced MRI was 1 mm or less and that the slice thickness was 2.5 mm or less.^[9] Prior studies with dedicated breast computed tomography (bCT) have shown the ability to provide isotropic voxel dimensions of 0.273 mm or less.^[10-12] Even without contrast enhancement, desmoplastic reaction and density changes can be discerned with bCT and clinical studies have shown an improvement in visualizing soft-tissue abnormalities with bCT compared to mammography.^[12-14] To our knowledge, there have been no prior reports investigating the use of dedicated bCT for monitoring NAC response. Hence, this prospective pilot study was conducted to determine the feasibility of non-contrast dedicated bCT as an imaging tool to determine primary tumor volume and monitor its changes during NAC.

MATERIALS AND METHODS

Human subjects

This prospective study was conducted in adherence to a Health Insurance Portability and Accountability Act-compliant,

institutional review board-approved protocol. Any woman who was recommended for NAC was eligible to participate in the study. All study participants provided written informed consent. Twelve women consented to participate in this pilot feasibility study, which is closed for accrual, of which one participant elected to undergo mastectomy in lieu of NAC and was excluded. Prior to initiation of NAC, 10 of the 11 study participants had a breast MRI exam (one subject had a FDG-PET exam) for extent-of-disease evaluation as part of standard-of-care. The tumor size from breast MRI, breast density from mammography assessed as per the American College of Radiology BI-RADS[®] criteria, receptor status, diagnosis from histopathology, and the drug combination used for NAC are summarized in Table 1.

Imaging protocol

All study participants were imaged using a clinical prototype dedicated bCT system (Koning Corporation, West Henrietta, NY, USA). The system uses a tungsten-anode X-ray tube operating at 49 kVp, an amorphous silicon flat-panel detector, and acquires 300 projections covering 360° in 10 s.^[10-12] The mean glandular dose (MGD) from a bCT scan is similar to and within the range from diagnostic mammography.^[11] The study participant was positioned prone on the patient support table with slight oblique rotation to facilitate inclusion of the axillary region and the breast was pendant through the aperture in the table. The manufacturer-provided filtered-back projection algorithm was used to reconstruct the breast at isotropic voxel size of 0.273 mm. All studies were performed without administration of contrast media.

The imaging protocol called for each study participant to undergo non-contrast bCT exams of the ipsilateral breast containing the index lesion at three time-points: Pre-treatment- before starting NAC; mid-treatment- after 4 cycles of doxorubicin (Adriamycin) and cyclophosphamide (Cytoxan) and before 4 cycles of either paclitaxel (Taxol) or the combination of 12 weekly cycles of paclitaxel (Taxol) and trastuzumab (Herceptin) for those who were Her2-neu positive; and, post-treatment- after completion of NAC. Of the 11 women who were enrolled in the study and underwent NAC, 2 study participants did not appear for their mid-treatment bCT exam. Where analysis permitted, bCT volumes from these two study participants were included.

Radiologist's segmentation

The reconstructed breast volumes were displayed on a 3-D workstation (Visage 7; Visage Imaging Inc., San Diego, CA, USA) provided with the bCT system. The workstation facilitates viewing of the breast volume in any desired orientation and includes tools for image manipulation

Table 1: Summary of study participants' data

ID	Pre-treatment		Receptor status [‡]			NAC drug combination [§]	Pathology	
	BD [†]	MRI size (cm)	ER	PR	HER2		Diagnosis*	Size [¶] (cm)
1	E	3.3 × 2.8 × 2.9	P	N	N	ACT	IDC	3
2	H	4.3 × 4.1 × 4.4	P	P	P	ACTH	IDC	0.1
3	H	7.4 × 2.7 × 5.4	N	N	N	ACT	IDC	4.8
4	S	No MRI	P	P	P	ACTH	IDC	0
5	S	3.3 × 2.2 × 2.0	P	P	P	ACTH	IDC	0.4
6	H	3.7 × 2.0	P	P	E	ACT	IDC	2.8
7	H	2.5	P	P	P	ACTH	IDC	0.8
8	H	6 × 8 × 9	P	P	N	ACT	ILC	0.8
9	E	4.6 × 3.7 × 4.5	N	N	N	ACT	IDC	0
10	S	9.2 × 10 × 11.7	N	P	N	ACT	IDC	0
11	E	5 × 4 × 4.5	N	N	N	ACT	IDC	2

[†]BD: mammographic breast density; S: Scattered fibroglandular; H: Heterogeneously dense; E: Extremely dense; [‡]Receptor status; ER: Estrogen receptor; PR: Progesterone receptor; HER2: Human epidermal growth factor 2; P: Positive; N: Negative; E: Equivocal; [§]NAC drug combination: ACT: Doxorubicin (Adriamycin); cyclophosphamide (Cytoxan); paclitaxel (Taxol); ACTH: ACT+trastuzumab (Herceptin); *Diagnosis: IDC: Invasive ductal carcinoma; ILC: Invasive lobular carcinoma; [¶]Size for the largest focus of invasive tumor after NAC and surgery (0 cm indicates complete pathological response for invasive tumor)

and quantitative analysis. A single radiologist (study author) marked the tumor boundary in multiple coronal views, from which the workstation computed the tumor volume [Figure 1]. The tumor volume from radiologist's manual segmentation served as the reference for comparison with the estimate from automated segmentation.

Automated segmentation

An automated segmentation algorithm (MatLab[®] version 8.1, The MathWorks Inc., Natick, MA, USA) was developed [Figure 2] by partly utilizing techniques for segmenting breast tissue in tomographic images.^[10,15] The skin layer was removed so as to minimize the possibility of skin being classified as tumor, when the tumor is at breast periphery.^[16] For the pre-treatment bCT exam, the algorithm leveraged the tumor location indicated by the biopsy clip. After excluding the coronal slices that contained the biopsy clip to mitigate beam-hardening artifacts, the breast volume was divided into regions posterior and anterior to the clip. Since the biopsy clip was 3 mm in size, a total of 11 slices, each 0.273 mm thick, were excluded. A bilateral filter was applied to each region for edge-preserving noise reduction prior to segmentation.^[17] Each region was segmented using two iterations of Kernel-based fuzzy c-means algorithm.^[18] The first iteration classified the breast volume into adipose and non-adipose tissues, and the second iteration used the non-adipose tissue volume to classify it into fibroglandular and cancerous tissues. The biopsy clip location was translated to the boundary of the posterior and anterior regions and served as a location-seed for a volume-growing algorithm applied to the cancerous tissue. The tumor volume was determined after interpolating for the slices that were excluded due to the clip. The mid-treatment and post-treatment bCT exams were registered with the pre-treatment bCT exam using 3D slicer,^[19] as the biopsy clip may migrate over time. The tumor from mid-treatment and post-treatment bCT exams was segmented in a similar manner as the pre-treatment

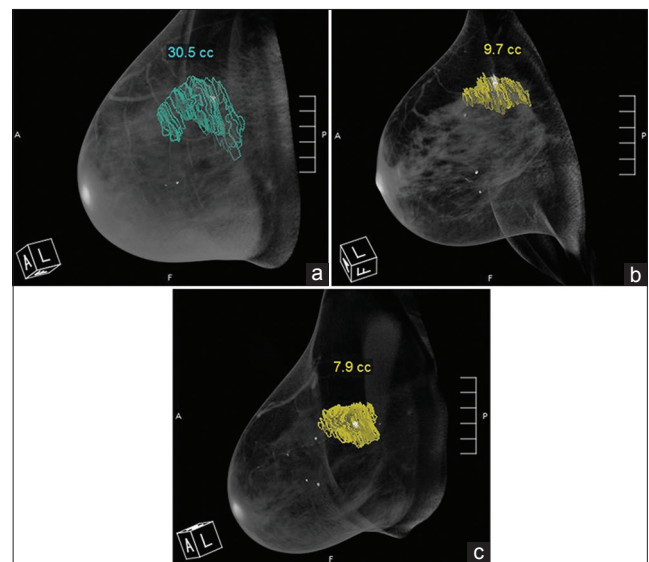


Figure 1: 48-year-old woman diagnosed with invasive ductal carcinoma. Radiologist segmented the tumor from multiple coronal images. Volume-rendered (3-D) breast CT images show the tumor volume obtained at (a) pre-treatment, (b) mid-treatment, and (c) post-treatment.

bCT exam. Once the tumor was segmented, an automated algorithm was used to determine the largest extent of tumor (size) in the sagittal plane that corresponds to the manner in which the specimen is sectioned by pathology to determine concordancy with pathology. An example of the segmented tumor is shown in Figure 3.

Statistical analysis

Parametric or non-parametric tests (SAS 9.3; SAS Institute Inc., Cary, NC, USA), depending on the results from normality test (Shapiro–Wilk test), were used to analyze the correlation in tumor volumes between the modalities (MRI and bCT) and between the segmentation methods (automated and manual). If the data did not satisfy the normality assumption, then logarithmic transform was attempted. The agreement was characterized by Bland–Altman plots. The influence of breast density

Algorithm for tumor segmentation
1. Skin thickness estimation and removal
2. Identify biopsy clip
3. Exclude coronal slices with clip
4. Divide breast into 2 volumes: anterior and posterior to clip
5. For each volume:
5a. Apply bilateral filter
5b. 1st KFCM iteration: segment to adipose and non-adipose tissue
5c. 2nd KFCM iteration: segment non-adipose tissue to fibroglandular and tumor
5d. Translate biopsy clip to volume boundary
5e. Use volume-growing algorithm with this location-seed
5f. Connected region represents the tumor
6. Interpolate for slices excluded due to clip

Figure 2: The automated algorithm with two iterations of kernel-based fuzzy c-means (KFCM) segmentation.

on the estimated tumor volume was also investigated. The correlation between the tumor sizes obtained from post-treatment bCT and from pathology was determined. Effects associated with $P < 0.05$ were considered statistically significant.

RESULTS

Comparison of automated and manual segmentation of bCT images

The distribution of the difference in tumor volumes between manual and automated segmentations after grouping over all three time points (pre-, mid-, and post-treatment) did not satisfy the normality assumption (Shapiro–Wilk test, $P=0.043$) and needed logarithmic transformation. Subsequent analyses reported in this section use log-transformed tumor volumes. Tumor volumes from automated and manual segmentations ($n = 31$ bCT scans) were correlated (Pearson's $r = 0.935$, $P < 0.001$). Result from the linear regression analysis is shown in Figure 4a, along with the identity line (dashes). The analysis showed high coefficient of determination ($r^2 = 0.875$), and the fit-parameters indicated a non-zero intercept and a slope less than unity. Hence, a Bland–Altman plot [Figure 4b] was generated which showed good agreement with most of the data points located within the limits of agreement (± 1.96 standard deviation) and a mean difference close to zero. The possibility that breast

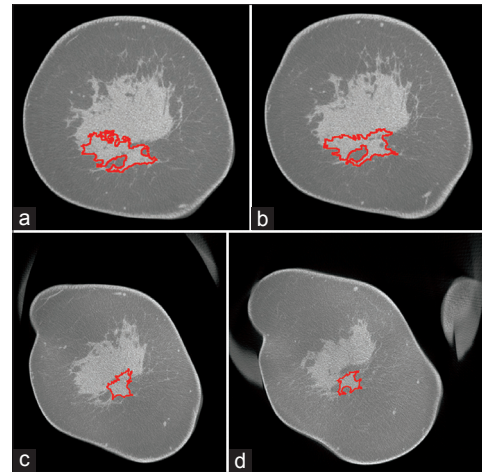


Figure 3: 41-year-old woman diagnosed with invasive ductal carcinoma at 6-o'clock position. (a–d) Cross-sectional (coronal) slices from post-treatment bCT exam performed prior to surgery show the contour (red) of the tumor segmented using the developed algorithm. The slices progress from the nipple toward the chest wall. The largest tumor dimension (size) was estimated over all sagittal planes that correspond to the manner in which the surgical specimen is sectioned by pathology. Tumor size determined using the algorithm was 2.82 cm. Pathology reported tumor size of 3 cm.

density could influence the automated segmentation was investigated. The percent difference in tumor volume was computed as, $\left[\frac{(V_{MbCT} - V_{AbCT})}{V_{MbCT}} \right] \times 100\%$, where V_{MbCT} and V_{AbCT} are the log-transformed tumor volumes from manual and automated segmentations, respectively. This metric was not statistically different among the breast density categories (Kruskal–Wallis test, $P = 0.169$). Repeated measures analysis of variance (ANOVA) indicated that the segmentation methods (automated or manual) did not have a statistically significant effect on the tumor volumes ($P = 0.808$) and that the changes in tumor volume over time were not dependent on the segmentation method (Wilk's lambda, $P = 0.316$). As expected, changes in tumor volume over the course of NAC were statistically significant ($P < 0.001$).

Correlation with pre-treatment breast MRI

The tumor size from the pre-treatment breast MRI ($n = 10$ subjects) interpretation report [Table 1] was used to estimate the tumor volume based either on ellipsoidal approximation for tumor shape when two or more dimensions were reported or on spherical approximation when only one dimension was reported. The pre-treatment tumor volume from MRI was compared with the pre-treatment tumor volume from bCT that was obtained by averaging the estimates from automated and manual segmentations. After logarithmic transformation, the tumor volumes satisfied the normality assumption (Shapiro–Wilk test, $P > 0.316$). Log-transformed tumor volumes from MRI and bCT were statistically correlated (Pearson's $r = 0.905$, $P < 0.001$). Linear regression analysis [Figure 5a] showed high coefficient of determination ($r^2 = 0.819$), slope approaching unity (0.933), and a non-zero intercept (-0.124). The Bland–

Altman plot [Figure 5b] showed good agreement with all the data points located within the limits of agreement (± 1.96 standard deviation). However, the mean difference was substantially different from zero. Hence, the influence of mammographic breast density was investigated. The percent difference in tumor volumes between MRI and bCT was calculated in a manner similar to above and did not exhibit a statistical difference among the breast density categories (Kruskal–Wallis test, $P = 0.312$).

Correlation with histopathology

Histopathology results indicated that three subjects had no residual invasive tumor, one subject had invasive ductal carcinoma (IDC) with microscopic foci of 0.8 and 1 mm, and one subject had a 4 mm residual IDC. The presence of biopsy clip (3 mm) in all subjects and

associated beam-hardening artifacts in bCT limited the ability to measure tumors of size approaching that of the biopsy clip. Hence, tumors smaller than 5 mm, which correspond to the upper bound for pT1, a primary tumor classification,^[20] were excluded from the analysis. Also, pathology report indicated that one subject had scattered foci of residual invasive lobular carcinoma (ILC) in three quadrants spanning approximately 16 cm, of which the largest focus was 8 mm. The tumor size determined from bCT for this subject was 9.5 cm. Limiting the analysis to IDC of size larger than 5 mm ($n = 5$ subjects), tumor size from post-treatment bCT was statistically correlated with pathology (Pearson's $r = 0.987$, $P = 0.002$). Also, the post-treatment tumor volume (log-transformed) from bCT was statistically correlated with tumor size from pathology (Pearson's $r = 0.908$, $P = 0.033$) for this

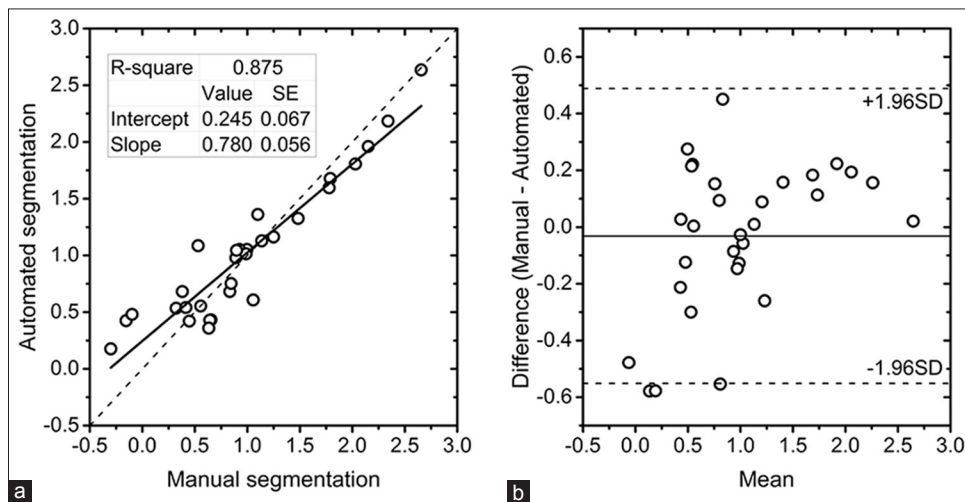


Figure 4: (a) Linear regression analysis of tumor volumes from automated and radiologist's manual segmentation. (b) Bland–Altman plot showing the agreement in tumor volumes between automated and manual segmentation. The tumor volumes are after logarithmic transformation.

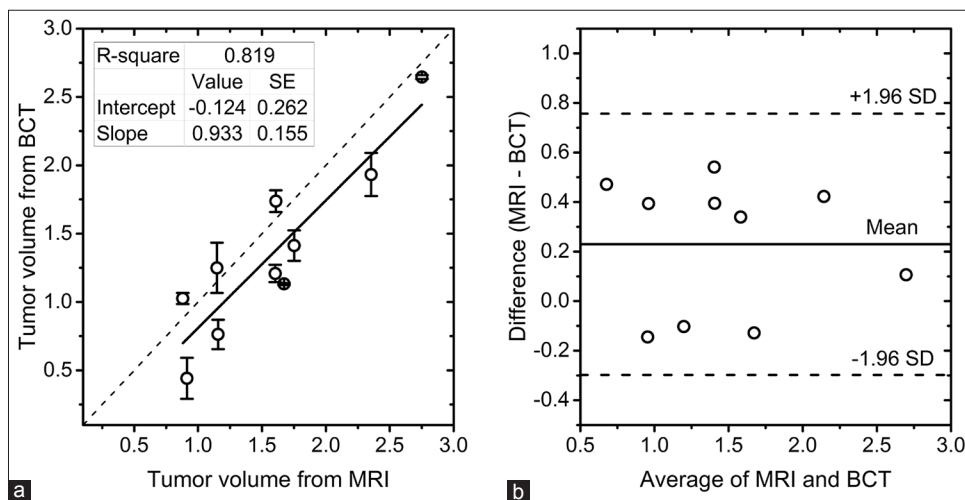


Figure 5: (a) Linear regression analysis of pre-treatment tumor volumes from MRI and bCT. The tumor volumes from bCT are represented by the mean and ± 1 standard deviation of the estimates from automated and radiologist's segmentations. (b) Bland–Altman plot showing the agreement in tumor volumes between MRI and bCT. The tumor volumes are after logarithmic transformation.

sub-group. Prior studies investigating concordance in tumor size between pathology and imaging modalities have used thresholds of 0.5, 1, and 2 cm.^[21-23] Applying the median threshold from these studies (1 cm), all subjects in this sub-group (ILC and pT1a or smaller excluded) were concordant [Figure 6] and the maximum difference in tumor size between pathology and post-treatment bCT was 0.57 cm for a subject assigned pT1b with 0.8 cm IDC.

Temporal changes in tumor size and volume

Temporal changes in tumor volume (log-transformed) determined using bCT from pre-treatment to mid-treatment and from mid-treatment to post-treatment are shown in Figure 7a and b, respectively. The tumor volumes from bCT at each time point were obtained by averaging the estimates

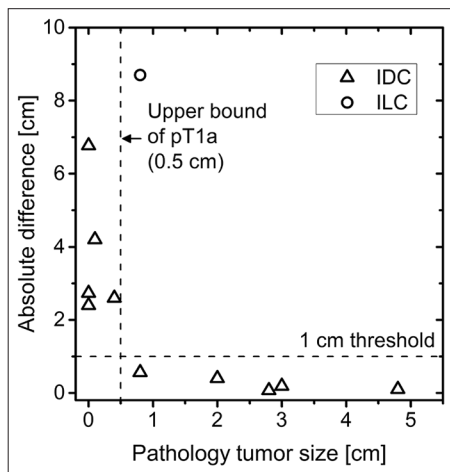


Figure 6: The absolute difference in tumor size between post-treatment bCT and pathology is plotted as a function of tumor size from pathology. For invasive ductal carcinoma (IDC) and for tumors larger than 0.5 cm (upper bound of pT1a primary tumor classification), tumor size from bCT was concordant with pathology at 1 cm threshold.

from automated and manual segmentations. The identity line is included for visual analysis. Reduction in tumor volume was observed at mid-treatment [Figure 7a] and was statistically different from pre-treatment tumor volume (paired *t*-test, $P = 0.0003$). The intercept from the linear regression analysis indicates that the tumor volume reduction averaged across all nine subjects who appeared for mid-treatment bCT was 47% ($1 - 10^{-0.273}$). Adapting the Response Evaluation Criteria in Solid Tumors (RECIST 1.1) which is intended for tumor size, all study participants who appeared for the mid-treatment bCT exam experienced at least a 30% reduction in tumor volume from pre-treatment.^[24] A further reduction in tumor volume from mid-treatment to post-treatment (paired *t*-test, $P = 0.002$) is observed in Figure 7b and the reduction averaged over all subjects was 34%. Comparison of the largest tumor dimension from pre-treatment MRI with the tumor size from pathology showed a reduction in tumor size for all subjects, indicating qualitative agreement with the temporal volume changes observed with bCT. Pathology confirmed partial ($n = 8$ subjects) or complete ($n = 3$ subjects) response for invasive tumor. The proportion of subjects with pathologic complete response was 27.3% (3/11) for subjects treated with doxorubicin (Adriamycin), cyclophosphamide (Cytosan), paclitaxel (Taxol) (ACT) drug combination [Table 1] and is similar to the 26% reported in NSABP-B27 trial.^[25]

DISCUSSION

Prior studies have used fuzzy c-means based approach for segmenting bCT images to skin, adipose, and fibroglandular tissue.^[10,26] It has been shown to be accurate to within $\pm 1.9\%$ in estimating the volume of an irregular shaped object.^[10] However, the presence

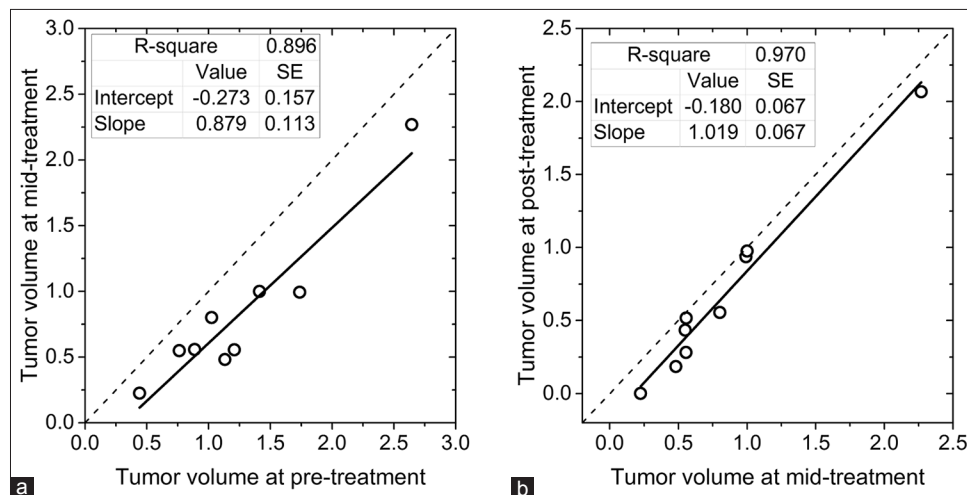


Figure 7: Temporal changes in tumor volume determined using bCT (a) from pre-treatment to mid-treatment and (b) from mid-treatment to post-treatment. Tumor volumes are after logarithmic transformation. All study participants experienced either partial or complete pathologic response. Reduction in tumor volume could be observed at mid-treatment with bCT.

of biopsy clip in all subjects limits the ability of the algorithm to determine tumor volume approaching the size of the clip. This results in slope less than unity in the linear regression analysis [Figure 4a]. Excluding the three smallest tumors and repeating the linear regression analysis improved the slope to 0.873 and intercept to 0.077. Referring to Figure 4a, the tumor volume from automated segmentation was higher than the manual (radiologist's) segmentation for the three smallest tumors, suggesting that the beam-hardening artifacts from the biopsy clip had less influence on radiologist's segmentation. The beam-hardening artifacts from the biopsy clip can be suppressed by metal-artifact reduction algorithms.^[27] This could potentially improve the accuracy for estimating the volume of smaller tumors and will be investigated in future.

In the absence of multifocal or multicentric disease, ultrasound is often used for extent-of-disease evaluation. However, ultrasound has lower sensitivity than MRI and underestimates the tumor size compared to MRI.^[22,28] A recent study of 149 cancers reported that the concordance and correlation with pathology was highest for MRI and was better than mammography, ultrasound, or digital breast tomosynthesis.^[29] Hence, the choice of MRI as reference standard for comparison with bCT for extent-of-disease evaluation is appropriate. Comparison of tumor volumes from pre-treatment breast MRI and bCT indicated a negative intercept in the linear regression analysis [Figure 4a] and a mean difference of 0.23 in the Bland–Altman plot [Figure 4b]. This implies that the tumor volume from bCT was smaller compared to MRI. Overestimation of tumor size by MRI compared to pathology has been reported.^[22,23] It has also been noted that the contrast (Gd) enhancement of the *in situ* component associated with the invasive tumor could be the source of overestimation with breast MRI.^[22] Also, the tumor volume from MRI was based on ellipsoidal or spherical approximation of tumor size from interpretation reports, as 3/10 subjects underwent breast MRI at institutions not associated with the study. Future studies will implement an MRI segmentation algorithm.

A search of the PubMed database did not identify any prior reports investigating the use of *dedicated bCT* for monitoring NAC response or for evaluating tumor size. However, there have been several studies using contrast-enhanced conventional (chest) CT to assess NAC response for breast cancer and to determine the tumor size.^[30-35] In a study of 285 patients with unifocal invasive breast carcinoma, 80% concordance with pathology at 5 mm threshold was observed with contrast-enhanced chest CT.^[35] One study comparing contrast-enhanced and non-contrast chest CT

for visualization of known breast tumors concluded that contrast enhancement is not needed to visualize known tumors in most patients.^[36] One major advantage with dedicated bCT compared to conventional CT is that the radiation dose is limited primarily to the breast with the rest of the body receiving minimal dose.^[37] This is of particular importance if contrast enhancement and the determination of perfusion parameters were to be pursued, which seem to be of value in predicting the response to NAC with conventional chest CT.^[34]

It is also important to consider the radiation dose from bCT in the context of subsequent treatment. Post NAC, patients undergo either mastectomy or breast conserving surgery followed by whole breast radiation therapy depending on the effectiveness of NAC and other factors.^[38] For patients who undergo mastectomy, the radiation-associated risk from bCT is negligible. For patients who undergo breast conserving surgery, radiation therapy delivers 40–50 Gy.^[39] This is 2 orders of magnitude higher or more than the cumulative dose from the three bCT scans. It is also relevant to note that the consensus statement on the use of accelerated partial breast irradiation (APBI) recommended that patients who underwent NAC should not receive APBI outside of a clinical trial due to lack of sufficient data.^[40] Thus, the radiation-associated risk from dedicated bCT for monitoring NAC response is minimal.

Limitations

The primary limitation of this study was the small sample size. This pilot study with a small number of study participants was intended to demonstrate the feasibility of non-contrast bCT to measure tumor volume (size) and monitor its changes during NAC. The results from this feasibility study show promise and indicate that a larger study is warranted. Additional limitations of the study were that the tumor volume was determined by a single radiologist and that the tumor volume from MRI was based solely on the radiologist's report and not from segmentation. A larger study is planned that would include concurrent breast MRI and dedicated bCT at each time point and measurements of tumor volume (size) by multiple radiologists to determine inter-observer variability.

CONCLUSION

In summary, this prospective study investigated the feasibility of non-contrast bCT as an imaging tool to determine primary tumor volume and monitor its changes during NAC. An automated segmentation algorithm was developed and tumor volumes from the automated segmentation were correlated with

radiologist's segmentation. Considering the study did not use contrast enhancement, the observations of reduction in tumor volume at mid-treatment in pathology-assessed responders, and statistical correlation and concordance in tumor size between bCT and pathology at post-treatment for tumors (IDC) larger than 5 mm are suggestive of potential benefits. This suggests that contrast enhancement may not be necessary for all subjects and needs further validation. Also, the observation that a larger reduction in tumor volume occurred between pre-treatment and mid-treatment than between mid-treatment and post-treatment suggests that bCT may be of value in predicting NAC response by mid-treatment. A larger study is needed to determine if tumor volume changes observed with bCT are predictive of pathologic response. The data also indicate that correction for beam-hardening effects from biopsy clip (if present) is needed to evaluate the size of smaller tumors. While this study investigated the feasibility of bCT for monitoring NAC response, some of the observations may also be applicable for evaluating tumor size for diagnostic imaging and surgical planning. The encouraging results from this feasibility study indicate that it would be of value to pursue larger studies.

ACKNOWLEDGMENTS

This work was supported in parts by the US Army Medical Research and Materiel Command grant W81XWH-09-1-0441 to Koning Corporation with sub-award to the University of Rochester Medical Center, and National Institutes of Health (NIH) grant R21CA176470 to the University of Massachusetts Medical School. The contents are solely the responsibility of the authors and do not represent the views of the funding agencies.

REFERENCES

1. Fisher B, Brown A, Mamounas E, Wieand S, Robidoux A, Margolese RG, et al. Effect of preoperative chemotherapy on local-regional disease in women with operable breast cancer: Findings from National Surgical Adjuvant Breast and Bowel Project B-18. *J Clin Oncol* 1997;15:2483-93.
2. Fisher B, Bryant J, Wolmark N, Mamounas E, Brown A, Fisher ER, et al. Effect of preoperative chemotherapy on the outcome of women with operable breast cancer. *J Clin Oncol* 1998;16:2672-85.
3. Wolmark N, Wang J, Mamounas E, Bryant J, Fisher B. Preoperative chemotherapy in patients with operable breast cancer: Nine-year results from National Surgical Adjuvant Breast and Bowel Project B-18. *J Natl Cancer Inst Monogr* 2001;96-102.
4. Chagpar AB, Middleton LP, Sahin AA, Dempsey P, Buzdar AU, Mirza AN, et al. Accuracy of physical examination, ultrasonography, and mammography in predicting residual pathologic tumor size in patients treated with neoadjuvant chemotherapy. *Ann Surg* 2006;243:257-64.
5. Rousseau C, Devillers A, Sagan C, Ferrer L, Bridji B, Campion L, et al. Monitoring of early response to neoadjuvant chemotherapy in stage II and III breast cancer by [18F] fluorodeoxyglucose positron emission tomography. *J Clin Oncol* 2006;24:5366-72.
6. Jung SY, Kim SK, Nam BH, Min SY, Lee SJ, Park C, et al. Prognostic Impact of [18F] FDG-PET in operable breast cancer treated with neoadjuvant chemotherapy. *Ann Surg Oncol* 2010;17:247-53.
7. De Los Santos JF, Cantor A, Amos KD, Forero A, Golshan M, Horton JK, et al. Magnetic resonance imaging as a predictor of pathologic response in patients treated with neoadjuvant systemic treatment for operable breast cancer. *Translational Breast Cancer Research Consortium trial 017. Cancer* 2013;119:1776-83.
8. Partridge SC, Gibbs JE, Lu Y, Esserman LJ, Tripathy D, Wolverton DS, et al. MRI measurements of breast tumor volume predict response to neoadjuvant chemotherapy and recurrence-free survival. *AJR Am J Roentgenol* 2005;184:1774-81.
9. Hylton NM, Blume JD, Bernreuter WK, Pisano ED, Rosen MA, Morris EA, et al. Locally advanced breast cancer: MR imaging for prediction of response to neoadjuvant chemotherapy—results from ACRIN 6657/I-SPY TRIAL. *Radiology* 2012;263:663-72.
10. Vedantham S, Shi L, Karellas A, O'Connell AM. Dedicated breast CT: Fibroglandular volume measurements in a diagnostic population. *Med Phys* 2012;39:7317-28.
11. Vedantham S, Shi L, Karellas A, O'Connell AM, Conover DL. Personalized estimates of radiation dose from dedicated breast CT in a diagnostic population and comparison with diagnostic mammography. *Phys Med Biol* 2013;58:7921-36.
12. O'Connell A, Conover DL, Zhang Y, Seifert P, Logan-Young W, Lin CF, et al. Cone-beam CT for breast imaging: Radiation dose, breast coverage, and image quality. *AJR Am J Roentgenol* 2010;195:496-509.
13. Lindfors KK, Boone JM, Nelson TR, Yang K, Kwan AL, Miller DF. Dedicated breast CT: Initial clinical experience. *Radiology* 2008;246:725-33.
14. O'Connell AM, Kawakyu-O'Connor D. Dedicated cone-beam breast computed tomography and diagnostic mammography: Comparison of radiation dose, patient comfort, and qualitative review of imaging findings in BI-RADS 4 and 5 lesions. *J Clin Imaging Sci* 2012;2:7.
15. Vedantham S, Shi L, Karellas A, Michaelsen KE, Krishnaswamy V, Pogue BW, et al. Semi-automated segmentation and classification of digital breast tomosynthesis reconstructed images. *Conf Proc IEEE Eng Med Biol Soc* 2011;2011:6188-91.
16. Shi L, Vedantham S, Karellas A, O'Connell AM. Technical note: Skin thickness measurements using high-resolution flat-panel cone-beam dedicated breast CT. *Med Phys* 2013;40:031913.
17. Paris S, Kornprobst P, Tumblin J, Durand F. Bilateral filtering: Theory and applications. *Found Trends Comp Graphics and Vision* 2009;4:1-73.
18. Bezdek JC, Keller J, Krisnapuram R, Pal NR. *Fuzzy Models and Algorithms for Pattern Recognition and Image Processing*. New York, NY: Springer Science+Business Media; 2005.
19. Fedorov A, Beichel R, Kalpathy-Cramer J, Finet J, Fillion-Robin JC, Pujol S, et al. 3D Slicer as an image computing platform for the Quantitative Imaging Network. *Magn Reson Imaging* 2012;30:1323-41.
20. American Joint Committee on Cancer (AJCC). *Breast*. In: Edge SB, Byrd DR, Compton CC, Fritz AG, Greene FL, Trotti A, editors. *AJCC Cancer Staging Manual*. 7th ed. New York, NY: Springer; 2010. p. 345-76.
21. Francis A, England DW, Rowlands DC, Wadley M, Walker C, Bradley SA. The diagnosis of invasive lobular breast carcinoma. Does MRI have a role? *Breast* 2001;10:38-40.
22. Berg WA, Gutierrez L, Ness-Aiver MS, Carter WB, Bhargavan M, Lewis RS, et al. Diagnostic accuracy of mammography, clinical examination, US, and MR imaging in preoperative assessment of breast cancer. *Radiology* 2004;233:830-49.
23. Onesti JK, Mangus BE, Helmer SD, Osland JS. Breast cancer tumor size: Correlation between magnetic resonance imaging and pathology measurements. *Am J Surg* 2008;196:844-50.
24. Eisenhauer EA, Therasse P, Bogaerts J, Schwartz LH, Sargent D, Ford R, et al. New response evaluation criteria in solid tumours: Revised RECIST guideline (version 1.1). *Eur J Cancer* 2009;45:228-47.

25. Rastogi P, Anderson SJ, Bear HD, Geyer CE, Kahlenberg MS, Robidoux A, et al. Preoperative chemotherapy: Updates of National Surgical Adjuvant Breast and Bowel Project Protocols B-18 and B-27. *J Clin Oncol* 2008;26:778-85.
26. Yang X, Wu S, Sechopoulos I, Fei B. Cupping artifact correction and automated classification for high-resolution dedicated breast CT images. *Med Phys* 2012;39:6397-406.
27. van der Bom IM, Hou SY, Puri AS, Spilberg G, Ruijters D, van de Haar P, et al. Reduction of coil mass artifacts in high-resolution flat detector conebeam CT of cerebral stent-assisted coiling. *AJNR Am J Neuroradiol* 2013;34:2163-70.
28. Gruber IV, Rueckert M, Kagan KO, Staebler A, Siegmann KC, Hartkopf A, et al. Measurement of tumour size with mammography, sonography and magnetic resonance imaging as compared to histological tumour size in primary breast cancer. *BMC Cancer* 2013;13:328.
29. Luparia A, Mariscotti G, Durando M, Ciatto S, Bosco D, Campanino PP, et al. Accuracy of tumour size assessment in the preoperative staging of breast cancer: Comparison of digital mammography, tomosynthesis, ultrasound and MRI. *Radiol Med* 2013;118:1119-36.
30. Inoue T, Tamaki Y, Hamada S, Yamamoto S, Sato Y, Tamura S, et al. Usefulness of three-dimensional multidetector-row CT images for preoperative evaluation of tumor extension in primary breast cancer patients. *Breast Cancer Res Treat* 2005;89:119-25.
31. Kanazawa T, Akashi-Tanaka S, Iwamoto E, Takasugi M, Shien T, Kinoshita T, et al. Diagnosis of complete response to neoadjuvant chemotherapy using diagnostic imaging in primary breast cancer patients. *Breast J* 2005;11:311-6.
32. Cheung YC, Chen SC, Hsieh IC, Lo YF, Tsai HP, Hsueh S, et al. Multidetector computed tomography assessment on tumor size and nodal status in patients with locally advanced breast cancer before and after neoadjuvant chemotherapy. *Eur J Surg Oncol* 2006;32:1186-90.
33. Tozaki M, Kobayashi T, Uno S, Aiba K, Takeyama H, Shioya H, et al. Breast-conserving surgery after chemotherapy: Value of MDCT for determining tumor distribution and shrinkage pattern. *AJR Am J Roentgenol* 2006;186:431-9.
34. Li SP, Makris A, Gogbashian A, Simcock IC, Stirling JJ, Goh V. Predicting response to neoadjuvant chemotherapy in primary breast cancer using volumetric helical perfusion computed tomography: A preliminary study. *Eur Radiol* 2012;22:1871-80.
35. Ahn SJ, Kim YS, Kim EY, Park HK, Cho EK, Kim YK, et al. The value of chest CT for prediction of breast tumor size: Comparison with pathology measurement. *World J Surg Oncol* 2013;11:130.
36. Boersma LJ, Hanbeukers B, Boetes C, Borger J, Ende Pv, Haaren Ev, et al. Is contrast enhancement required to visualize a known breast tumor in a pre-operative CT scan? *Radiother Oncol* 2011;100:271-5.
37. Sechopoulos I, Vedantham S, Suryanarayanan S, D'Orsi CJ, Karellas A. Monte Carlo and phantom study of the radiation dose to the body from dedicated CT of the breast. *Radiology* 2008;247:98-105.
38. Morrow M, Strom EA, Bassett LW, Dershaw DD, Fowble B, Giuliano A, et al. American College of Radiology; American College of Surgeons; Society of Surgical Oncology; College of American Pathology. Standard for breast conservation therapy in the management of invasive breast carcinoma. *CA Cancer J Clin* 2002;52:277-300.
39. Smith BD, Bentzen SM, Correa CR, Hahn CA, Hardenbergh PH, Ibbott GS, et al. Fractionation for whole breast irradiation: An American Society for Radiation Oncology (ASTRO) evidence-based guideline. *Int J Radiat Oncol Biol Phys* 2011;81:59-68.
40. Smith BD, Arthur DW, Buchholz TA, Haffty BG, Hahn CA, Hardenbergh PH, et al. Accelerated partial breast irradiation consensus statement from the American Society for Radiation Oncology (ASTRO). *Int J Radiat Oncol Biol Phys* 2009;74:987-1001.

Source of Support: None of the authors have financial interests pertaining to this study. At the time of writing this article, the Koning Breast CT had received CE Mark approval in Europe and Health Canada approval, but is not US FDA approved for clinical use,
Conflict of Interest: None declared.